



Lawrence Berkeley Laboratory

UNIVERSITY OF CALIFORNIA

Materials & Chemical Sciences Division

National Center for Electron Microscopy

Presented at the Materials Research Society Fall Meeting,
Boston, MA, November 28–December 3, 1988

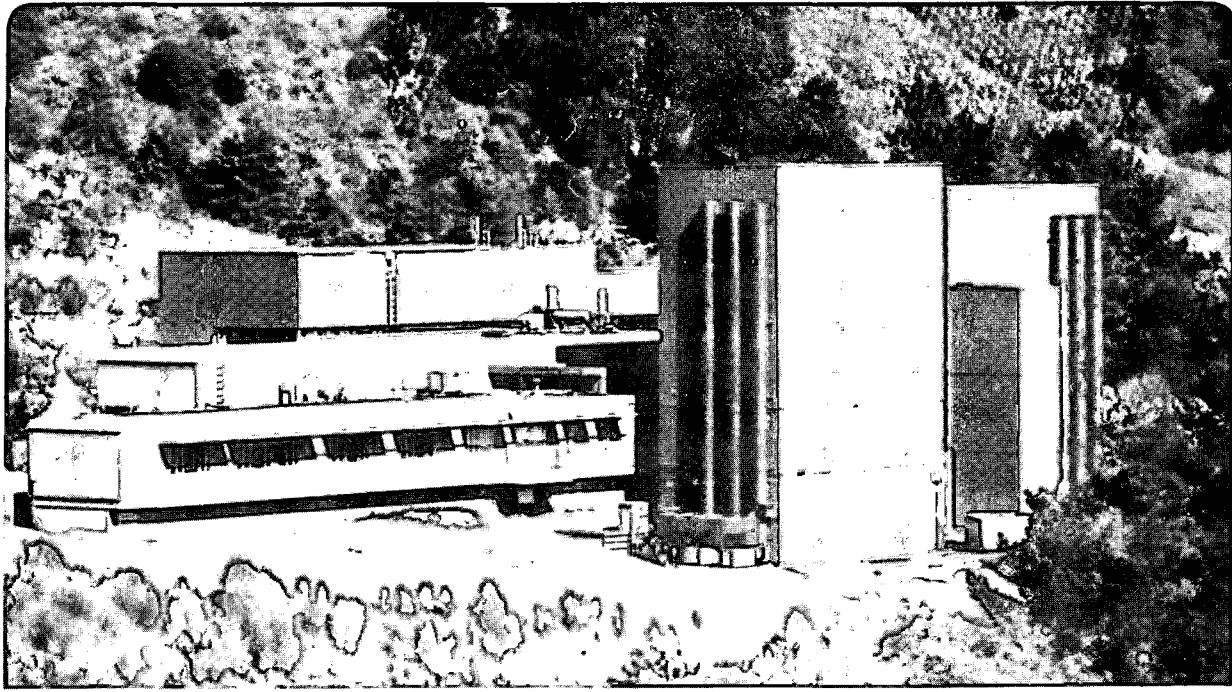
RECEIVED
LAWRENCE
BERKELEY LABORATORY
JUN 6 1989

LIBRARY AND
DOCUMENTS SECTION

The Berkeley Atomic Resolution Microscope — an Update

C.J.D. Hetherington, E.C. Nelson, K.H. Westmacott,
R. Gronsky, and G. Thomas

March 1989



LBL-25797
c.2

DISCLAIMER

This document was prepared as an account of work sponsored by the United States Government. While this document is believed to contain correct information, neither the United States Government nor any agency thereof, nor the Regents of the University of California, nor any of their employees, makes any warranty, express or implied, or assumes any legal responsibility for the accuracy, completeness, or usefulness of any information, apparatus, product, or process disclosed, or represents that its use would not infringe privately owned rights. Reference herein to any specific commercial product, process, or service by its trade name, trademark, manufacturer, or otherwise, does not necessarily constitute or imply its endorsement, recommendation, or favoring by the United States Government or any agency thereof, or the Regents of the University of California. The views and opinions of authors expressed herein do not necessarily state or reflect those of the United States Government or any agency thereof or the Regents of the University of California.

THE BERKELEY ATOMIC RESOLUTION MICROSCOPE - AN UPDATE.

C.J.D. HETHERINGTON, E.C. NELSON, K.H. WESTMACOTT, R. GRONSKY, AND G. THOMAS.

National Center for Electron Microscopy, Lawrence Berkeley Laboratory, University of California, 1 Cyclotron Rd., Berkeley, CA 94720.

ABSTRACT

Recent modifications to the JEOL ARM-1000 microscope have markedly enhanced its performance. The point resolution limit at 1000kV is confirmed by optical diffractograms down to 1.7Å and there are firm indications of contrast transfer down to 1.4Å. The unique tilting capability of the ARM, $\pm 40^\circ$ biaxial tilt over the 800kV to 1000kV range, is preserved at this resolution. This paper presents the measured imaging parameters and results of resolution tests.

INTRODUCTION

The Atomic Resolution Microscope (or JEOL ARM-1000) was installed at Lawrence Berkeley Laboratory in 1983. The design represented a major advance in high resolution instrumentation and some of its features are still unique. Over the last year its performance has been investigated and some improvements have been made. The purpose of this paper is to report on this work and to demonstrate the capabilities of the ARM using results from recent projects.

First, the concepts behind the ARM are described (for further information, see refs. [1,2]). The high resolution is achieved primarily by using high accelerating voltages while keeping C_s low. The top entry'specimen stage has a height control which allows the value of $C_s\lambda$ to be held constant at all voltages. The height control, rather than the objective lens current, also serves as a coarse focus control. This preserves the microscope alignment to a large extent which is convenient when minimising radiation damage under the beam. Above 600kV, the long focal lengths of the objective lens mean that very large tilts of the sample holders are made possible. Mechanical vibration isolation from the surroundings is provided by a system designed by Korfund Dynamics consisting of a 100 ton inertia block mounted on airbags.

Second, some recent developments are outlined. Low level mechanical vibrations originating in turbo pumps, cooling fans and water recirculators were identified and suppressed. A Gatan image intensifier was installed which has made operation of the ARM more accurate, more efficient and swifter; this, again, helps reduce beam damage. (Incidentally, the intensifier's first YAG crystal showed surprisingly little damage after 12 months of operation.) On-line

digitisation and analysis of images by the NCEM computer facility are now possible. A beam tilt wobbler [3,4] has been installed that gives a more accurate beam alignment than the original voltage centering method; this is demonstrated by, for example, the occurrence of half-spacing fringes in images. The reliability of the ARM is much improved so that over the last two years, downtime (mostly preplanned maintenance) has been below the 10% level.

MEASUREMENTS OF IMAGING PARAMETERS

C_s and λ

The undamped contrast transfer function (CTF) is determined by C_s and λ ; these parameters were measured on the ARM at 800 and 1000kV and are recorded in table I. The theoretical point resolution is defined here as the spatial frequency at which the transfer drops to a certain level ($\chi = -\pi/4$). In fact, instabilities reduce the transfer to that level at a much lower spatial frequency and they limit the resolution of the ARM. So the objective lens design on the ARM combined with the increased accelerating voltage mean that C_s and λ do not limit the microscope's performance. The undamped and damped transfer functions (shown in figure 2) are discussed later. One further parameter that is related to the CTF is the finest focus step which was measured to be around 45Å.

Even though the low values of C_s and λ are not critical to the point resolution of the ARM, they do affect a microscope's performance in other ways. At the sample, shorter wavelengths slightly increase the extinction distances. Secondly, there is less spreading of the electron waves by Fresnel diffraction since the scattering angles are smaller. Thirdly, the ratio of inelastic to elastic scattering is smaller at higher voltages. And, of course, knock-on damage increases. At the lens, a shorter λ increases the Fourier period of lattice images [6]. A small value of C_s allows the same spatial coherence to be obtained using a larger beam divergence. This is another justification for having such a low value of C_s on the ARM for it helps ensure sufficient illumination for high resolution work.

Mechanical Stability

The suppression of mechanical vibrations to a satisfactory level is demonstrated in figure 1 which is an image of gold particles taken under tilted illumination showing fringes of spacing 1.2Å. Similarly, half-spacings in small unit cell structures such as aluminum are regularly visible. On the ARM, this has had a considerable effect not only on the second order (g, -g) image details, but

also on the linear (0, g) image details and has therefore directly improved the resolution limit. Thus the sub-1.7Å contrast transfer described later can now be detected.

Beam Divergence

Condenser aperture sizes are chosen so that the beam divergence semi-angles at 800 and 1000kV do not limit the contrast transfer at Scherzer defocus. A 150µm aperture gives a semi-angle of 0.55mrad at 1000kV and a 100µm aperture gives a semi-angle of 0.76mrad at 800kV (these are equivalent to semi-angles of 1.04 and 1.24mrad respectively at 400kV). From a more practical perspective, choice of aperture sizes is also based on the effect of the beam intensity on exposure times and on specimen damage.

Energy Spread

It seems that the energy spread is currently the most serious factor responsible for limiting the resolution of the ARM. It is also one of the parameters that is hardest to measure. The spread of focus which results from the damping can be estimated by matching simulated and experimental images or by comparing calculated CTF's with optical diffractograms. These exercises give a figure of around 150Å (at 1000kV) and the resulting chromatic envelope damps the CTF as shown in figure 2. The C_c has been measured at around 3mm (1000kV) and the relative contributions of the different instabilities to the energy spread are currently under investigation.

MICROSCOPE PERFORMANCE

Resolution

The point resolution is defined as the highest spatial frequency at which contrast from a weak phase object is transferred linearly at optimum defocus. The actual limit of transfer is typically taken as either $\sin\chi = 0$ ("first zero") or $\sin\chi = -0.707$. On a standard HREM, the damping does not reduce the level of transfer at this spatial frequency and the point resolution limit is easily defined given C_s and λ . However, on the ARM and on other high voltage HREM's (see for example [7,8]), the damping can have a significant effect on the transfer within the first zero, and a definition of the resolution limit requires a level-of-transfer criterion (as for information resolution limits).

We have not yet attempted an accurate quantification of the CTF but it does appear for the ARM that there is strong transfer down to around 1.7\AA and weaker transfer to around 1.4\AA . Figure 3 shows an image taken at around Scherzer defocus at 1000kV with its optical diffractogram (ODM). The cleaved sample of germanium is viewed down a $[125]$ zone axis and the crossed $\{311\}$ planes have spacings of 1.70\AA .

Figure 4 shows an image taken at around -550\AA defocus of a cleaved germanium sample in an orientation where only two $\pm\{400\}$ beams are strongly excited. The presence of the fringes means that there is still sufficient transfer at 1.41\AA for strongly diffracting lattice planes to appear in the image. (Thus, a gold lattice has been clearly imaged down $[111]$ using the $\{220\}$ planes of 1.44\AA spacing.)

The ODM of figure 5 is taken from a micrograph of the amorphous material found at the edge of an ion milled germanium sample. The crystalline spots ($\{311\}$ reflections) from thicker regions calibrate the ODM. At first sight, the lack of intensity beyond 1.7\AA is puzzling; however, the sharp cut off is partly explained by the fact that the ODM shows the power spectrum which is proportional to the square of $\sin\chi$, and partly by the decrease in scattering from this material at around 1.7\AA (as seen in diffraction patterns).

Tilt

The standard tilt holders have $\pm 40^\circ$ biaxial tilt, although the shortened focal lengths at 500 and 400kV restrict the tilt to 35° and 20° respectively. The two advantages of these large tilts are, firstly, that almost all samples can be tilted to the desired orientation, and secondly, that the same region can be lattice imaged down two or more zone axes. The maximum tilt of around $\pm 50^\circ$ is obtained midway between the tilt axes of the holder, allowing orthogonal zones to be viewed (see [9] for an example). Figure 6 is taken from a recent study of GaAs islands on Si [10]. The practical difficulties associated with such an experiment should be mentioned: the highly inclined sample means the region must be flat and thin, the stability of the holder must be excellent, the sample must not damage too much during the time required for tilting and the defocus varies rapidly across the micrograph.

Examples of recent applications

Three examples of recent applications of the ARM in the fields of semiconductors, metals and ceramic superconductors are shown in figures 6, 7 and 8.

SUMMARY

The point resolution of the ARM is demonstrated at 1.7\AA ; transfer down towards the first zero (1.3\AA at 1000kV) has been detected but it is weakened by chromatic error. The unique $\pm 40^\circ$ biaxial tilt stage means that the same sample can be examined down orthogonal directions. These capabilities are now being applied to research into metals, ceramics, semi- and superconductors.

ACKNOWLEDGEMENTS

The authors thank M.A. O'Keefe and D.J. Smith for useful discussions, J. Turner for photography and D. Ah Tye for sample preparation. The ARM is available to qualified microscopists at no cost for non-proprietary research. The ARM and the NCEM are supported by the Director, Office of Energy Research, Office of Basic Energy Science, Materials Science Division of the U.S. Department of Energy under contract No. DE-AC03-76SF00098.

REFERENCES

1. R. Gronsky, "38th Ann. Proc Electron Microscopy Soc. Amer.", p2 (San Francisco, California) G.W. Bailey (ed.) (1980)
2. H. Watanabe et al., "Proc. of 7th Int. Conf. on High Voltage Electron Microscopy", p5 (Lawrence Berkeley Laboratory, California) R.M. Fisher, R. Gronsky and K.H. Westmacott (eds.) (1983)
3. D.J. Smith et al., Ultramicroscopy, 11 pp263 - 282 (1983)
4. The beam tilt wobbler was built and installed by A. Higgs of Academ Co., 2136 E. Cornell, Tempe, AZ 85283
5. K. Tsuno and T. Honda, Optik, 64 p367 (1983)
6. S. Iijima and M.A. O'Keefe, J. of Microscopy, 117 p347 (1979)
7. M.A. O'Keefe in report by R.M. Fisher and T. Imura, Ultramicroscopy, 3 p3 (1978)
8. D.J. Smith et al., J. of Microscopy, 130 pp127 - 136 (1983)
9. R. Hull et al., Appl. Phys. Lett., 49 p1714 (1986)
10. F.A. Ponce and C.J.D. Hetherington, to be published.

| Voltage | 800kV | 1000kV |
|---|------------------|------------------|
| λ (nominal) | 0.01027Å | 0.00872Å |
| λ (measured ¹) | 0.01022±0.00006Å | 0.00865±0.00007Å |
| C_s (calculated ²) | 1.95mm | 2.3mm |
| C_s (measured ³) | 1.93±0.12mm | 2.27±0.22mm |
| Scherzer defocus ⁴ = $-\sqrt{1.5C_s\lambda}$ | -544Å | -543Å |
| theoretical pt. resln. ⁴ = $0.67 C_s^{1/4}\lambda^{3/4}$ | 1.43Å | 1.31Å |
| ¹ by Kikuchi band widths ² see [5] ³ by displacement between aligned and tilted beam in-focus images ⁴ using measured values of λ and C_s | | |

Table I.
Comparison of measured and calculated parameters on the ARM
at optimum objective lens currents.

FIGURE CAPTIONS

Figure 1. 1.2\AA fringes in a tilted beam image of gold particles (negative taken at 600,000x, 2 second exposure).

Figure 2. Actual (1) and undamped (2) CTF's at 1000kV.

Figure 3. Image with ODM of cleaved Ge, {311} planes. Note transfer to 1.7\AA .

Figure 4. Image with ODM of cleaved Ge, (400) planes. Note transfer at 1.4\AA .

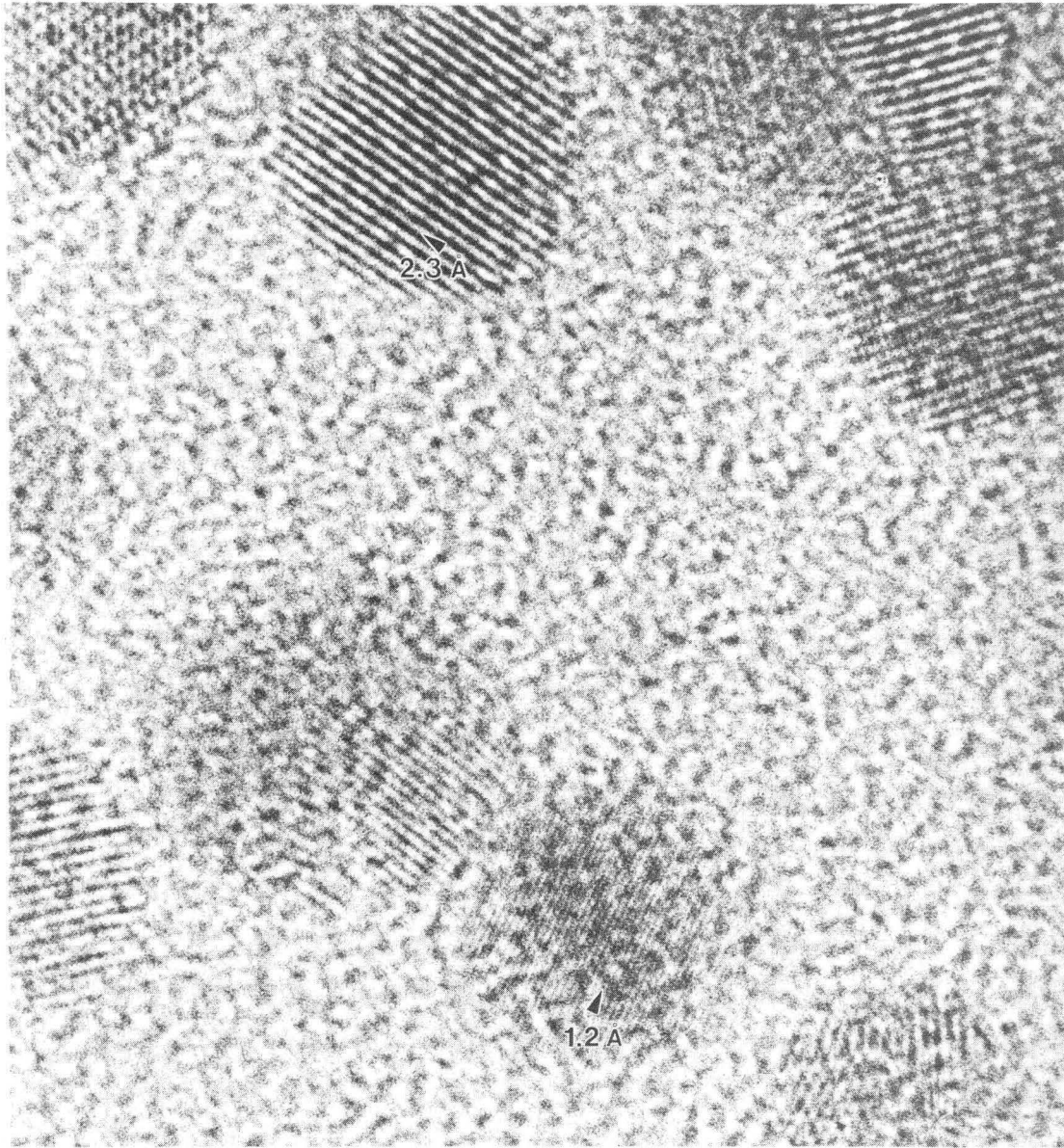
Figure 5. ODM at 1000kV, -550\AA defocus, amorphous Ge.

Figure 6 a) A GaAs island on (001)Si viewed down $[1\bar{1}0]$. The sample was prepared as a $[100]$ cross section and tilted $+45^\circ$.

b) The same GaAs island on (001)Si; here it is tilted -45° to be viewed down $[110]$. Note that the two images provide information on island morphology and defect distribution. Sample courtesy of Dr. F.A. Ponce, Xerox PARC.

Figure 7. A 90° $\langle 110 \rangle$ tilt boundary in aluminum in symmetrical orientation taken at 800kV, defocus $\sim -800\text{\AA}$. The arrows indicate the periodicity in the boundary. Sample courtesy of Dr I. Yamada, Kyoto University.

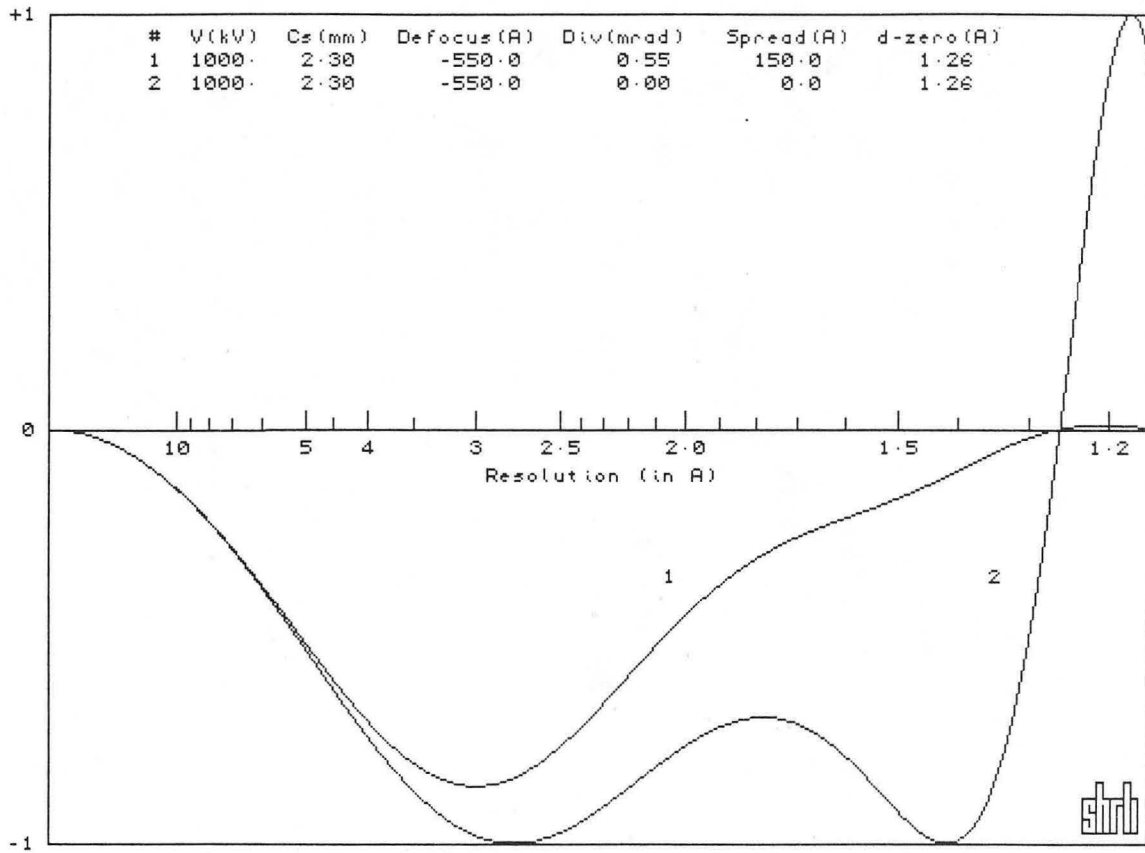
Figure 8. BiCaSrCuO superconductor prepared by cleaving and imaged at 800kV, defocus $\sim -550\text{\AA}$, in a $[110]$ orientation. Polytypoids with different numbers of Cu-O planes ($n = 2, 3$ and 4) are indicated. Sample courtesy of S.M. Green, U.C. San Diego.



XBB 891-589

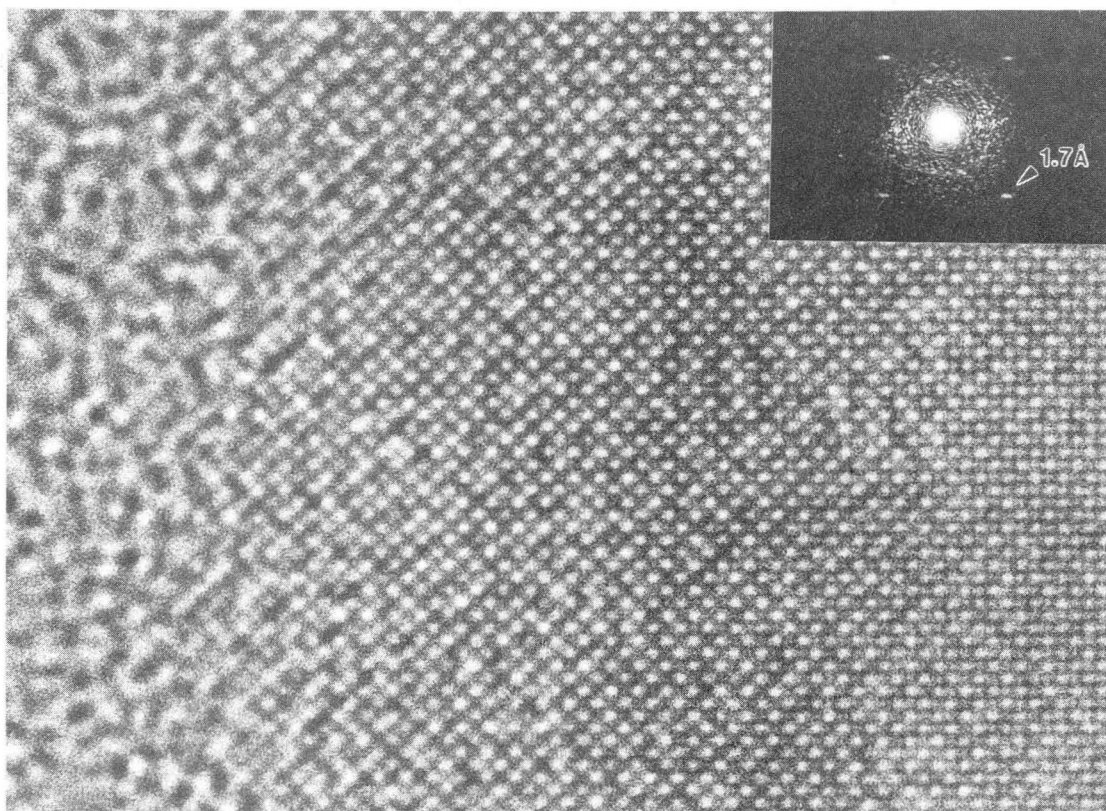
Fig. 1

SHRLI82A - FIRST-ORDER PHASE CONTRAST TRANSFER FUNCTION(S)



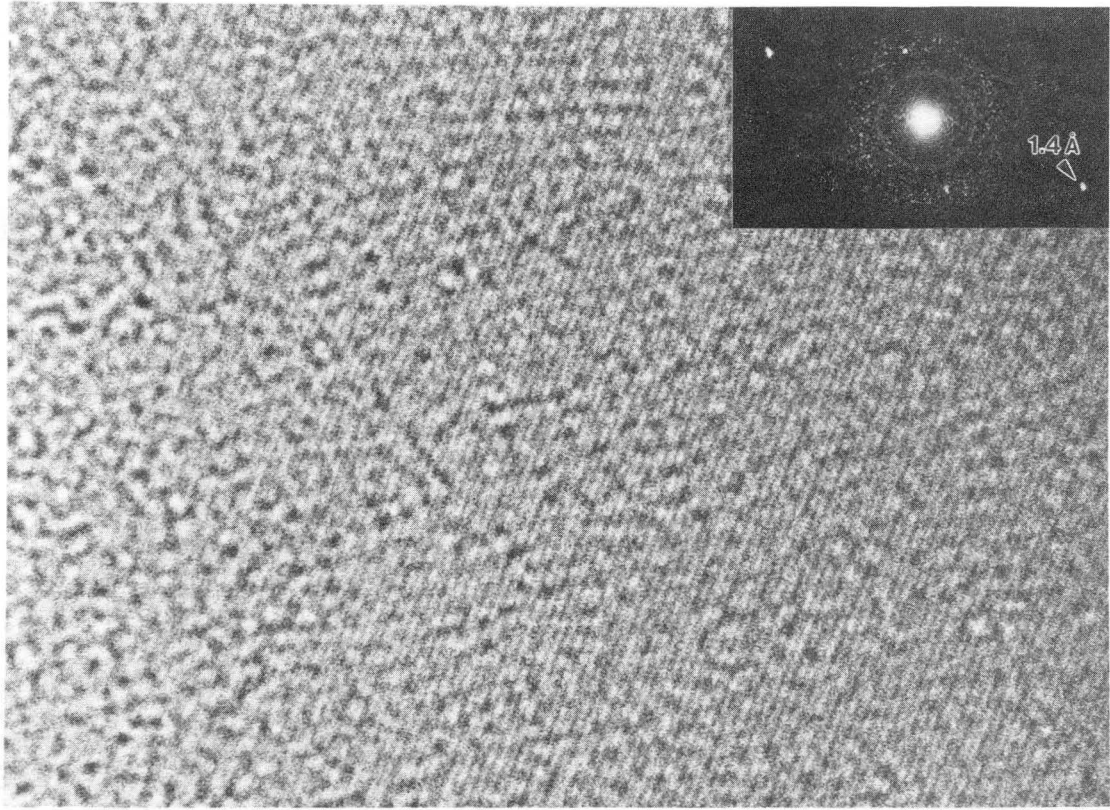
XBL 891-338

Fig. 2



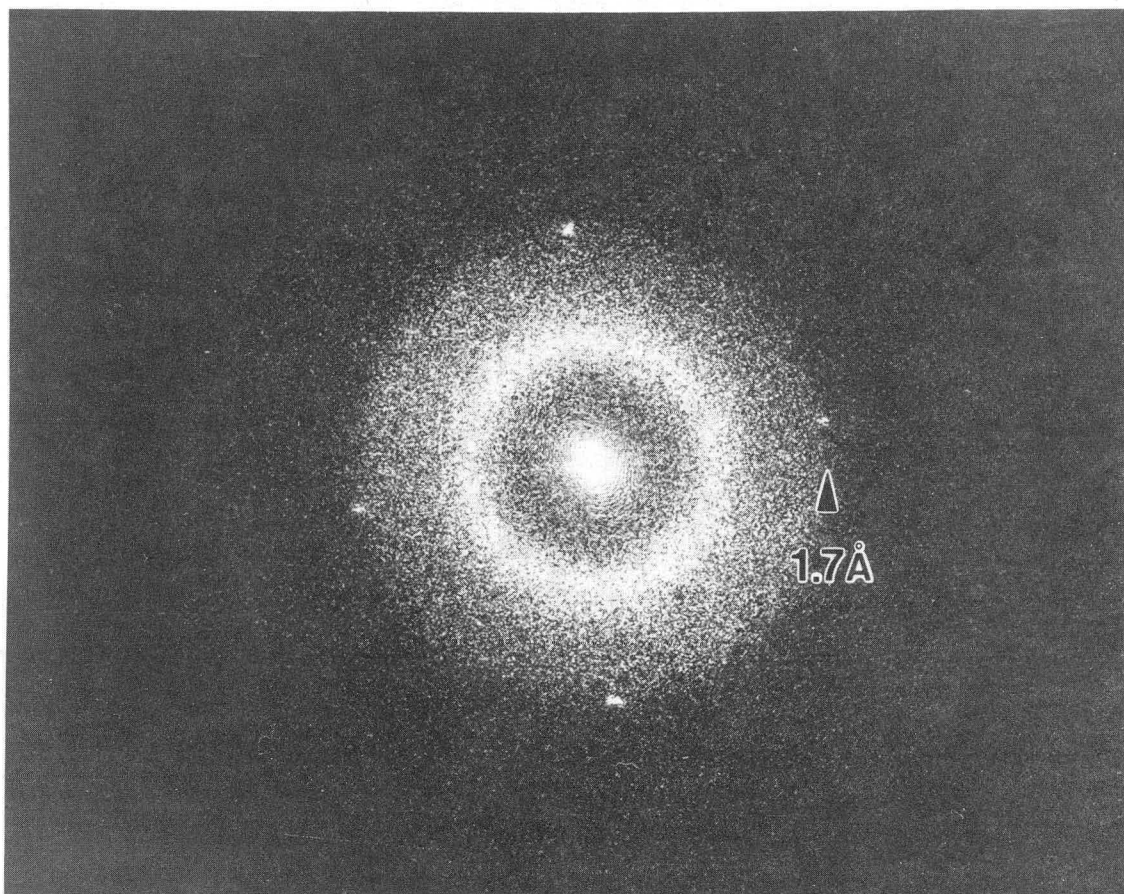
XBB 891-590

Fig. 3



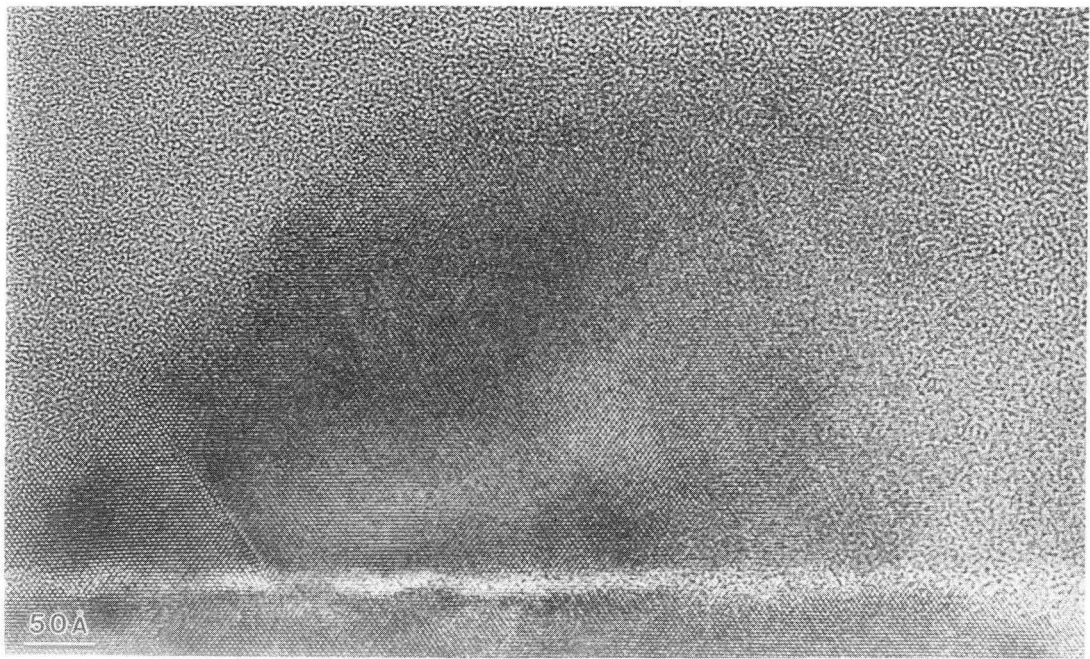
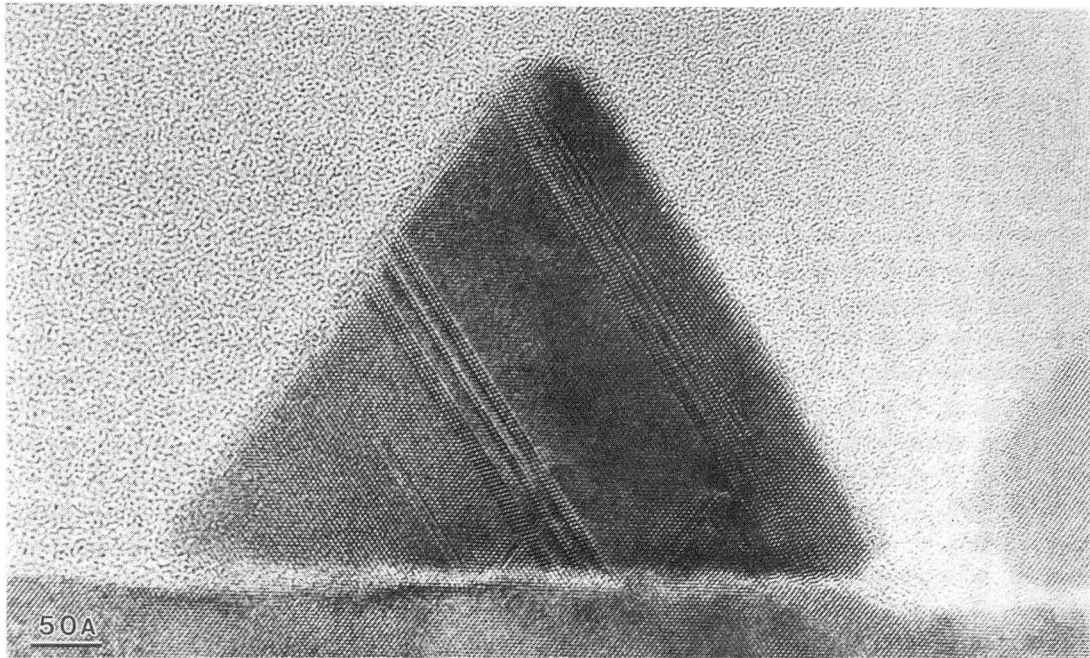
XBB 891-591

Fig. 4



XBB 891-592

Fig. 5



XBB 891-593

Fig. 6

XBB 880-10320

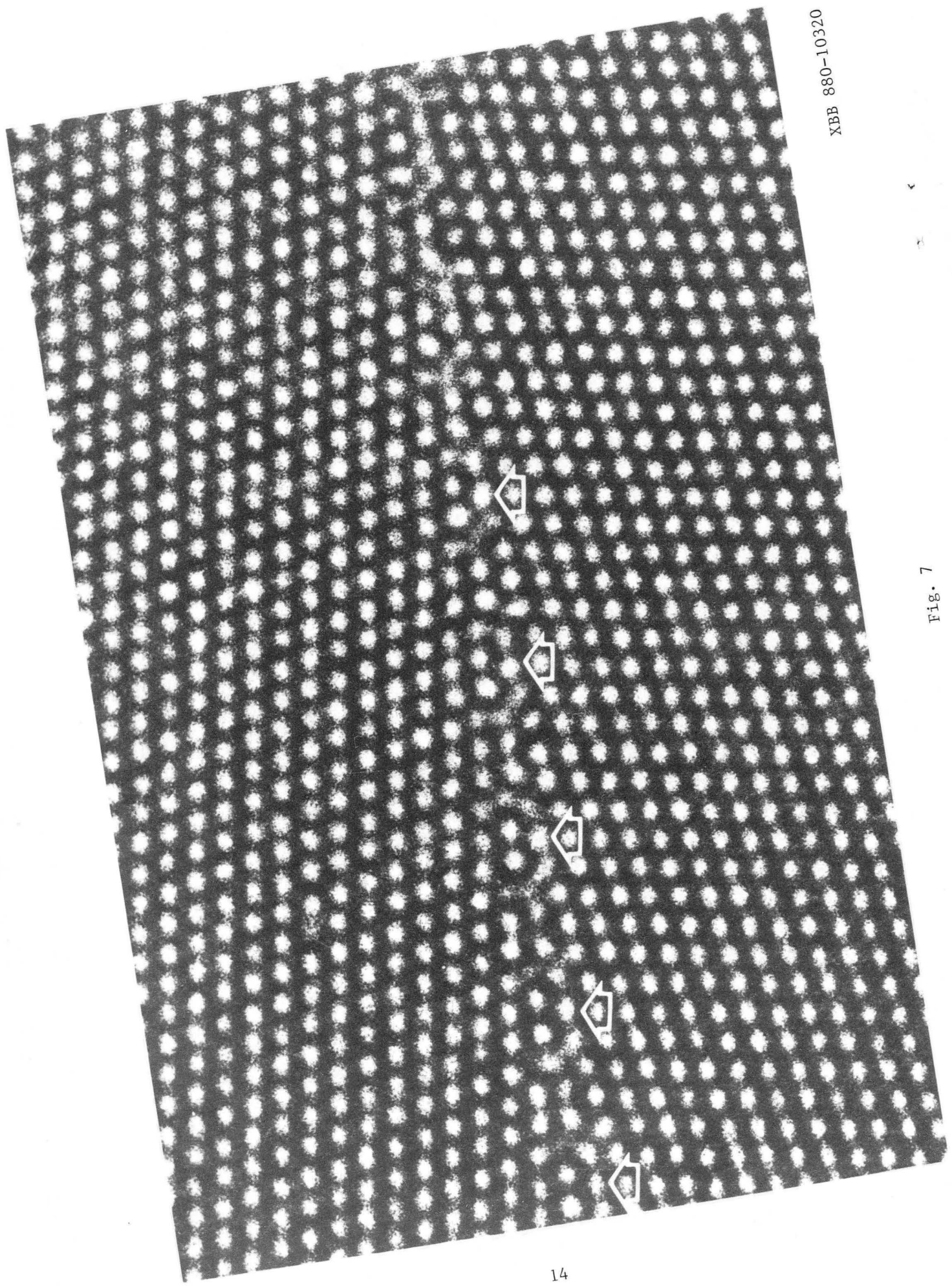
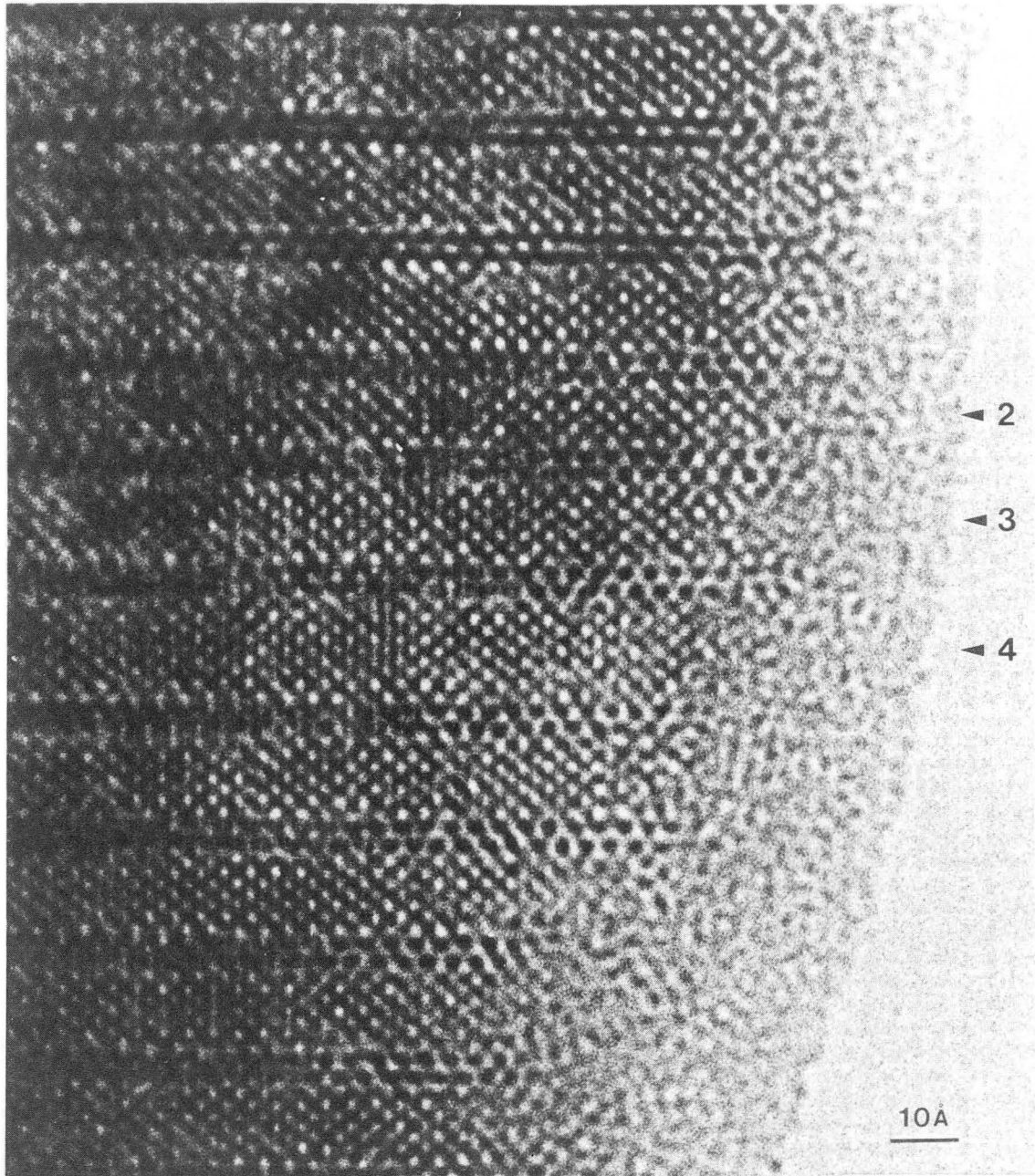


Fig. 7



XBB 891-594

Fig. 8

LAWRENCE BERKELEY LABORATORY
TECHNICAL INFORMATION DEPARTMENT
1 CYCLOTRON ROAD
BERKELEY, CALIFORNIA 94720